

1 **Research article**

2

3 **MicroRNA-125a/b Inhibits A20 and MAVS to Promote Inflammation and**  
4 **Impair Antiviral Response in Chronic Obstructive Pulmonary Disease**

5 Alan C-Y. Hsu<sup>1\*</sup>, Kamal Dua<sup>1</sup>, Malcolm R. Starkey<sup>1</sup>, Tatt-Jhong Haw<sup>1</sup>, Prema M. Nair<sup>1</sup>,  
6 Kristy Nichol<sup>1</sup>, Nathan Zammit<sup>2</sup>, Shane T. Grey<sup>2</sup>, Katherine J. Baines<sup>1</sup>, Paul S. Foster<sup>1</sup>, Philip  
7 M. Hansbro<sup>1†</sup>, and Peter A. Wark<sup>1,3†</sup>

8

9 <sup>1</sup>Priority Research Centre for Healthy Lungs, Hunter Medical Research Institute and The  
10 University of Newcastle, New South Wales, Australia.

11 <sup>2</sup>Transplantation Immunology Group, Immunology Division, Garvan Institute of Medical  
12 Research, Sydney, New South Wales, Australia

13 <sup>3</sup>Department of Respiratory and Sleep Medicine, John Hunter Hospital, Newcastle, New  
14 South Wales, Australia

15

16 \*Correspondence to: Dr Alan Hsu & Prof Phil Hansbro, Ph.D. Priority Research Centre for  
17 Healthy Lungs, Hunter Medical Research Institute, Lot 1 Kookaburra Circuit, New Lambton  
18 Heights, Newcastle, NSW 2305, Australia. Phone: +61 2 4042 0109; Fax: +61 2 4042 0046;  
19 Email: Alan.Hsu@newcastle.edu.au, Philip.Hansbro@newcastle.edu.au

20

21 The authors have declared that no conflict of interest exists.

22 Total word count for the body of the manuscript: 3,872

23

24 **ABSTRACT**

25 Influenza A virus (IAV) infections lead to severe inflammation in the airways. Patients with  
26 chronic obstructive pulmonary disease (COPD) characteristically have exaggerated airway  
27 inflammation and are more susceptible to infections with severe symptoms and increased  
28 mortality. The mechanisms that control inflammation during IAV infection and the  
29 mechanisms of immune dys-regulation in COPD are unclear. We found that IAV infections  
30 lead to increased inflammatory and antiviral responses in primary bronchial epithelial cells  
31 (pBECs) from healthy non-smoking and smoking subjects. In pBECs from COPD patients,  
32 infections resulted in an exaggerated inflammatory but deficient antiviral responses. A20 is an  
33 important negative regulator of nuclear factor-kappaB (NF- $\kappa$ B)-mediated inflammatory but not  
34 antiviral response, and A20 expression was reduced in COPD. IAV infection increased the  
35 expression of micro(miR)-125a/b, which directly reduced the expression of A20 and  
36 mitochondrial antiviral signaling (MAVS), and caused exaggerated inflammation and impaired  
37 antiviral responses. These events were replicated *in vivo* in a mouse model of experimental  
38 COPD. Thus, miR-125a/b and A20 and may be targeted therapeutically to inhibit excessive  
39 inflammatory responses and enhance antiviral immunity in IAV infections and in COPD.

40

## 41 INTRODUCTION

42 Influenza A viruses (IAVs) are amongst the most important infectious human pathogens that  
43 cause enormous morbidity and mortality worldwide. This largely results from seasonal  
44 influenza but an important feature of the biology of IAVs is the frequent emergence of novel  
45 pandemic strains/subtypes. Infections cause symptoms ranging from mild to severe viral  
46 pneumonia, with uncontrolled inflammation in the airways.

47         Bronchial epithelial cells (BECs) are the primary site of IAV infection, and innate  
48 immune responses produced by these cells are important in the early protection against the  
49 viruses (1, 2). During infection viral RNAs are recognized by toll-like receptor 3 (TLR3) and  
50 retinoic acid-inducible gene-I (RIG-I). Upon binding of TLR3 to viral RNAs signalling  
51 pathways are initiated that activate receptor interacting protein 1 (RIP1) by ubiquitination.  
52 Activated RIP1 indirectly phosphorylates I $\kappa$ B $\alpha$ , leading to the release of active p65 and p50  
53 subunits of nuclear factor-kappaB (NF- $\kappa$ B) into the nucleus where they induce the transcription  
54 of inflammatory genes including of cytokines such as interleukin-6 (IL-6), tumor necrosis  
55 factor- $\alpha$  (TNF- $\alpha$ ), and IL-1 $\beta$ , and chemokines such as CXC chemokine ligand-8 (CXCL-8/IL-  
56 8) (3-5). These inflammatory cytokines recruit immune cells, in particular macrophages and  
57 neutrophils, to the site of infection that phagocytose pathogens and apoptotic cells (6, 7). RIG-  
58 I interacts with mitochondrial antiviral-signaling protein (MAVS), which activates interferon  
59 regulatory factor 3 (IRF3) by phosphorylation. Activated IRF3 then translocates into the  
60 nucleus where it initiates the production of type I and III interferons (IFNs) (8, 9). These innate  
61 cytokines induce the transcription of over 300 IFN-stimulated genes (ISGs) including the Mx1  
62 protein that disrupts virus replication (10).

63         The control of inflammation is critical to achieving optimal inflammatory responses  
64 that clear viruses without excessive damage to host tissues and airways. We have previously  
65 shown that A20, also known as TNF- $\alpha$ -inducing protein 3 (TNFAIP3), is a negative regulator

66 of NF- $\kappa$ B-mediated inflammation that functions by targeting RIP1 for degradation, and  
67 therefore suppresses NF- $\kappa$ B activation (11-14). Micro-RNAs (miRNAs; miRs) are another  
68 important class of immune signaling regulators that silence gene expression by degradation  
69 (15). miR-125a and b have recently been shown to directly inhibit A20, leading to increased  
70 NF- $\kappa$ B activation (16). It is currently unknown if A20 or miR-125a/b regulates type I and III  
71 IFNs during IAV infections.

72       Chronic obstructive pulmonary disease (COPD) is the 3<sup>rd</sup> leading cause of illness and  
73 death globally and is characterized by progressive airway inflammation, emphysema, and  
74 reduced lung function (17). The most important risk factor for COPD in Western societies is  
75 cigarette smoking (18). COPD patients have increased susceptibility to IAV infections that  
76 cause acute exacerbations and result in more severe symptoms, disease progression, and  
77 increased mortality (19-21). Current therapeutics remain limited to vaccination and antiviral  
78 drugs. These have major issues with the constant need for developing new vaccines, COPD  
79 patients respond poorly to vaccination, IAVs have become drug resistant and all therapeutics  
80 have questions surrounding availability and efficacy in future pandemics (22, 23). There is  
81 therefore an urgent need to develop novel therapeutics for influenza, especially for those most  
82 susceptible to infection.

83       Despite inflammatory signalling pathways being well-characterized, the mechanisms  
84 underlying the exaggerated inflammatory responses to IAV, including in COPD are unclear. It  
85 is known that increased NF- $\kappa$ B activation is elevated in biopsies from COPD patients (24). We  
86 have previously shown that human influenza H3N2 infection induced heightened inflammatory  
87 responses (25), and high pathogenic avian H5N1 is known to induce severe cytokine storms in  
88 the lung (9, 26). We also showed that primary BECs (pBECs) from COPD subjects and our  
89 established *in vivo* model of experimental COPD have increased inflammatory and impaired  
90 antiviral responses to IAV infections, leading to more severe infection (27-29). Furthermore,

91 miRNAs are known to be altered in COPD (30, 31). However, the molecular mechanisms  
92 underpinning the heightened inflammatory response in IAV infections and defective immune  
93 responses in COPD remain unclear. In this study, we investigated the mechanisms involved  
94 using our established experimental systems (27, 32-34). We found that COPD pBECs and mice  
95 with experimental COPD infected with IAV have higher levels of inflammatory cytokines but  
96 reduced antiviral responses (30, 35). We uncovered that NF- $\kappa$ B-mediated inflammation in IAV  
97 infection and in COPD was also exaggerated, which resulted from decreased levels of A20  
98 protein, which in turn was caused by elevated levels of miR-125a/b. Treatment with specific  
99 antagomiRs against miR-125a or b reduced NF- $\kappa$ B activation but also increased type I and III  
100 IFNs production and suppressed infection. We then found that miR-125a and b directly targets  
101 MAVS 3' untranslated region (UTR), thereby suppressing the induction of type I/III IFNs. This  
102 study therefore discovers a novel miR-125-mediated pathway that reduces A20 and MAVS  
103 and promotes excessive inflammation and increases susceptibility to IAV infection in COPD.  
104 It also identifies novel potential therapeutic options that reduce IAV-mediated inflammation  
105 and reverse immune signaling abnormalities in COPD.

106           Some of the data has been previously reported in abstract form (36).

107

## 108 **RESULTS**

109

### 110 **IAV infection induces increased inflammatory but reduced antiviral responses *ex vivo* in** 111 **human COPD pBECs**

112 pBECs from healthy non-smoking control subjects, COPD patients (ex-smoker) or smoking  
113 (smoker) controls and were infected with IAV H3N2 or H1N1 (MOI 5). Virus replication was  
114 measured 24hr after infection. Virus titers increased at 24hr (Fig. 1A), and was two-fold greater  
115 in COPD pBECs compared to controls. Infection resulted in the production of the pro-

116 inflammatory cytokines/chemokines IL-6, CXCL-8, TNF- $\alpha$ , and IL-1 $\beta$ , and antiviral cytokines  
117 type I (IFN- $\beta$ ) and type III interferons (IFN- $\lambda$ 1) (Fig. 1B). In COPD, the induction levels of  
118 cytokines were substantially higher (2.5-10 fold) compared with healthy control and smoker  
119 pBECs (Fig. 1B). In contrast, the induction of IFN- $\beta$  and IFN- $\lambda$ 1 proteins were reduced in  
120 COPD.

121 We then measured the levels of activity of NF- $\kappa$ B by assessing the levels of phosphorylated  
122 p65 at Ser536 (phospho-p65) (35, 37, 38). Infection significantly increased the activation of  
123 p65 (phospho-p65) in both healthy and smoker pBECs at 6hr, which was further increased at  
124 24hr (Fig. 1C; Supplementary Fig. S1A). In COPD pBECs the protein levels of phospho-p65  
125 was elevated at baseline (media controls) at 6hr and significantly increased with infection at  
126 24hr compared to healthy and smoker controls.

127

### 128 **IAV infection also induces increased inflammatory but reduced antiviral responses *in*** 129 ***vivo* in experimental COPD**

130 We then demonstrated these events also occur *in vivo*. BALB/c mice were exposed to either  
131 normal air (Air) or cigarette smoke (Smk) for eight weeks. The Smk group develops hallmark  
132 features of COPD as previously described extensively (27, 28, 32-35, 39). Mice were then  
133 infected with IAV A/PR/8/34, and viral titers, airway inflammation (histopathological score),  
134 and inflammatory and antiviral cytokines were determined at 7 days post infection (dpi) (Fig.  
135 2A). Infection in Air-exposed controls leads to virus replication (Fig. 2B) that was  
136 accompanied by significant airway inflammation (histopathological score, Supplementary Fig.  
137 S1B). Infection in Smk-exposed mice resulted in a significantly higher virus titers (four-fold)  
138 and airway histopathological score (three fold) compared to Air-exposed mice. In support of  
139 these data, the levels of the pro-inflammatory cytokines/chemokines IL-6, KC (mouse  
140 equivalent of CXCL-8), TNF- $\alpha$ , and IL-1 $\beta$  were also increased by infection in Air- and to a

141 greater extent in Smk-exposed groups (Fig. 2C). Antiviral cytokines were increased in infected  
142 Air-exposed controls but were either not induced (IFN- $\beta$ ) or were induced to a much reduced  
143 level (IFN- $\lambda$ 3) in infected Smk-exposed groups (Fig. 2D). The exaggerated release of pro-  
144 inflammatory cytokines was associated with significantly increased levels of phospho-p65  
145 protein in infected Smk-exposed compared to Air-exposed controls (Fig. 2E; Supplementary  
146 Fig. S1C). In all experiments, ultraviolet-inactivated virus did not have any effects compared  
147 to media controls (data not shown).

148 Taken together these human *ex vivo* and experimental *in vivo* data demonstrate that IAV  
149 infections result in increased airway inflammation, pro-inflammatory and antiviral responses.  
150 However, COPD is associated with exaggerated inflammation and reduced antiviral responses,  
151 leading to increased virus replication.

152

153 **A20 is an important negative regulatory of NF- $\kappa$ B-mediated inflammatory but not**  
154 **antiviral responses, and its expression is reduced in human COPD and experimental**  
155 **COPD**

156 We have previously shown that A20 is an important negative regulator of NF- $\kappa$ B activation  
157 (11-14), but its roles during IAV infection and whether it also regulates the induction of type I  
158 and III IFNs is unclear. We hypothesized that A20 protein expression would be down-regulated  
159 and would contribute to the increased activation of NF- $\kappa$ B in response to IAV infection in  
160 COPD. IAV infection led to a significant induction of A20 protein at 6hr and 24hr in healthy  
161 and smoker controls, but this increase was impaired in COPD pBECs (Fig. 3A; Supplementary  
162 Fig. S2A). Similarly in Smk-exposed mice, A20 protein expression was reduced in airway  
163 epithelial cells compared to Air-exposed controls (Supplementary Fig. S2B).

164 We then investigated if A20 was important in NF- $\kappa$ B-mediated inflammatory responses, and if  
165 exaggerated p65 activation was the direct result of reduced A20 protein levels during infection

166 in COPD pBECs. We inhibited A20 expression using A20-specific siRNA 24hr before  
167 infection, and measured the activation of p65 and the production of pro-inflammatory  
168 cytokines/chemokines 24hr after infection. Inhibition of A20 expression (Fig. 3B;  
169 Supplementary Fig. S2C) resulted in significant increases in the protein levels of phospho-p65  
170 (Fig. 3C; Supplementary Fig. S2C), and pro-inflammatory cytokines/chemokines IL-6, CXCL-  
171 8, TNF- $\alpha$ , and IL-1 $\beta$  (Fig. 3D) compared to un-treated controls, whether pBECs were infected  
172 or not. Conversely, ectopic (ecto-) expression using a pcDNA-A20 expression vector reduced  
173 the phosphorylation of p65 (Supplementary Fig. S2D). Nevertheless, inhibition or ecto-  
174 expression of A20 did not affect IFN- $\beta$  and IFN- $\lambda$ 1 induction (Fig. 3E; Supplementary Fig.  
175 S2D). siRNA negative control or control vector did not affect the induction of A20 or phospho-  
176 p65 protein (Supplementary Fig. S2E-F).

177 Collectively these data indicate that A20 is an important negative regulator of NF- $\kappa$ B but is  
178 dispensible in the induction of type I and III IFNs. A20 protein expression is dysregulated in  
179 COPD.

180

### 181 **Elevated miR-125a and b levels decrease A20 levels, increase inflammation and impair** 182 **antiviral responses in COPD pBEC and experimental COPD**

183 miR-125a and b have recently been shown to directly target and inhibit A20 expression (16),  
184 but its roles during IAV infection and in COPD are unknown. Thus, we measured the levels of  
185 miR-125a and b induced by IAV infection. H3N2 and H1N1 infections resulted in significant  
186 increases in the levels of these miRs at 24hr in pBECs from all groups (Fig. 4A). However,  
187 their levels were substantially greater at baseline and during infection (2-4 fold) in COPD  
188 pBECs compared to healthy controls. We then confirmed the direct link between increased  
189 miR-125a and b levels and reduced A20 protein induction using specific antagomiRs and  
190 mimetics. pBECs were pre-treated with either miR-125a or b specific antagomiRs or mimetics

191 for 24hr before infection, and A20, phospho-p65, inflammatory and antiviral cytokines and  
192 were assessed 24hr after infection. AntagomiR treatment inhibited miR-125a or b expression  
193 (Supplementary Fig. S3A), and this resulted in significant increases in A20 protein production,  
194 reduced phosphorylation of p65, subsequent induction of pro-inflammatory  
195 cytokines/chemokines, and enhanced antiviral IFN- $\beta$  and  $\lambda$ 1 responses (Fig. 4B and  
196 Supplementary Fig. S3B-E) compared to un-treated controls. Conversely miR-125a or b  
197 mimetics decreased A20 protein induction, increased phospho-p65 protein levels and reduced  
198 IFN- $\beta$  responses (Supplementary Fig. S3F). Treatment with scrambled miR or mimetic  
199 controls did not affect A20, phospho-p65, or IFN- $\beta$  production (Supplementary Fig. S3G-H).

200 We then assessed whether similar events occurred *in vivo*. IAV infection significantly increased  
201 the levels of miR-125a and b in both groups, with the levels in Smk group significantly higher  
202 compared to Air-exposed controls (Fig. 4C). We then inhibited miR-125a or b before and  
203 during infection (Fig. 4D). We also extended the *ex vivo* data by inhibiting both miR-125a and  
204 b together. Treatment with miR-125a or b antagomiR, alone or in combination, reduced  
205 histopathological scores (Fig. 4E and Supplementary Fig. S4A) and improved lung function  
206 (reduced lung volume determined during a pressure-volume loop manoeuvre) in Air and Smk-  
207 exposed groups compared to infected scrambled antagomiR-treated controls (Supplementary  
208 Fig. S4B). Inhibition of miR-125a, b, or a and b, also increased A20 protein expression in the  
209 airway epithelium and decreased the levels of phospho-p65 compared to the controls (Fig. 4F;  
210 Supplementary Fig. S4C-D). Importantly while we could only detect reductions in TNF- $\alpha$  and  
211 KC with combined treatment (Supplementary Fig. S4E), antagomiR treatment, either alone or  
212 in combination, also significantly increased IFN- $\beta$  and IFN- $\lambda$ 3 protein induction (Fig. 4F and  
213 Supplementary Fig. S4D).

214 Collectively, these data show that miR-125a and b are directly involved in the regulation of  
215 both inflammatory cytokines, through the control of A20, and antiviral cytokine production  
216 through an unknown target.

217

### 218 **miR-125a and b target MAVS**

219 To determine the mechanism of miR-125a and b-mediated regulation of antiviral IFN- $\beta/\lambda$ , we  
220 performed miRNA prediction analysis using TargetScan ([www.targetscan.org](http://www.targetscan.org)). miR-125a and  
221 b have a putative binding site in the 3'-UTR of human and mouse *MAVS* (Fig. 5A-B). To  
222 examine these putative interactions we first assessed the protein levels of MAVS in pBECs.  
223 MAVS protein levels were significantly increased 24hr after IAV infection in healthy control  
224 and smoker, but notably not in COPD pBECs (Fig. 5C; Supplementary Fig. S5A). Similarly,  
225 infection in Smk-exposed mice was also associated with significantly impaired production of  
226 MAVS compared to infected Air-exposed controls at 7dpi (Fig. 5D; Supplementary Fig. S5B).  
227 To confirm the potential interaction of miR-125a/b and MAVS, we cloned the putative binding  
228 region of miR-125a and b in wild-type (MAVS-WT) or mutant (MAVS-MT) *MAVS* 3'-UTR  
229 into a luciferase reporter construct. The construct was co-transfected into HEK293 cells along  
230 with miR-125a or b mimetics, or scrambled controls, and then luciferase activity was assessed.  
231 Co-transfection of miR-125a or miR-125b mimetics with MAVS-WT resulted in a significant  
232 decrease in luciferase activity compared to scrambled controls (Fig. 5E). There was no  
233 reduction in activity with co-transfection with MAVS-MT. We then determined if *MAVS* gene  
234 is present with the miR-125a or b mimetics in the silencing complex. To do this we  
235 immunoprecipitated Argonaute 2 (Ago2), a core component of RNA-induced silencing  
236 complex (RISC) that binds to the miRNAs and their target mRNA, with a specific antibody  
237 and detected the presence of both *A20* and *MAVS* by qPCR, which could not be detected with

238 immunoprecipitation with IgG control (Fig. 5F). This confirmed that miR-125a and b directly  
239 bind to the endogenous 3'-UTR of *MAVS*.

240

## 241 **miR-125a and b targeting of MAVS regulates antiviral responses in COPD pBEC and** 242 **experimental COPD**

243 We then investigated whether inhibition of miR-125 has a functional outcome. We showed that  
244 miR-125a and b antagomiR treatment lead to significant increases in MAVS (Fig. 6A and  
245 Supplementary Fig. S6A-B), IFN- $\beta$  and IFN- $\lambda$ 1 protein induction (Fig. 4B and Supplementary  
246 Fig. S3C), and reduced viral replication in both healthy and control pBECs (Fig. 6B). In  
247 contrast, mimetics suppressed the induction of antiviral cytokines and increased virus titers  
248 (Supplementary Fig. S3F). Similarly in Smk-exposed mice, inhibition of miR-125a, b, or a+b  
249 resulted in increased induction of MAVS (Fig. 6C and Supplementary Fig. S6C), IFN- $\beta$  and  
250 IFN- $\lambda$ 3 (Fig. 4F and Supplementary Fig. S4D-E), and inhibited virus replication (Fig. 6D).

251 Collectively these data demonstrate that miR-125a and b negatively regulate MAVS expression  
252 and suppress the induction of IFN- $\beta/\lambda$ , and may potentially be targeted therapeutically in the  
253 prevention and/or treatment of IAVs and COPD.

254

## 255 **DISCUSSION**

256

257 Here we discover that IAV infections induce airway inflammation and antiviral responses,  
258 however in COPD pBECs and experimental COPD inflammatory responses and activation of  
259 NF- $\kappa$ B are exaggerated but antiviral responses are impaired. We show that A20 is a negative  
260 regulator of NF- $\kappa$ B-mediated induction of inflammatory but not antiviral cytokines, and that  
261 A20 protein levels were impaired in COPD. The impaired induction of A20 and antiviral  
262 responses in COPD was attributed to increased expression of miR-125a and b. Elevated levels

263 of these miRNAs suppressed A20 expression, leading to heightened NF- $\kappa$ B activity and  
264 inflammation and reduced antiviral responses. Inhibition with miR-125a and b antagomiRs  
265 increased A20 levels and reduced NF- $\kappa$ B activity, and also promoted IFN production. We then  
266 demonstrated that miR-125a and b modulated IFN induction by targeting MAVS translation.  
267 MAVS protein levels were reduced in COPD, but could be increased with specific miR-125a  
268 and b antagomiR treatment that also induced IFN production. Thus, IAV infection induces the  
269 expression of miR-125a/b that suppress A20 and MAVS, in turn promoting NF- $\kappa$ B-induced  
270 inflammation and attenuating antiviral IFN production, respectively, increasing viral  
271 replication. All these events are exaggerated in COPD (Fig. 7).

272 IAV is a major infectious pathogen that poses serious health concerns worldwide.  
273 Infections, particularly with highly pathogenic influenza viruses, cause severe airway  
274 inflammation and a cytokine storm with high morbidity and mortality. COPD is a major global  
275 health problem that is underpinned by exaggerated inflammatory responses in the airways (40).  
276 IAV infections frequently result in acute exacerbations of COPD, leading to accelerated  
277 declines in lung function (41, 42) and increased mortality (20). The mechanisms of exaggerated  
278 inflammation and severe outcomes in COPD are poorly understood, and there are no effective  
279 therapies for these events.

280 Here we show that IAV-mediated inflammatory response are dampened with ectopic  
281 expression of A20 that reduces NF- $\kappa$ B activity and inflammatory responses, without affecting  
282 type I and III IFN responses. A20 is a de-ubiquitinating enzyme that degrades RIP1 and inhibits  
283 NF- $\kappa$ B activation (13), and has been shown to suppress the induction of IFN- $\beta$  (43). We found  
284 that A20 modulated NF- $\kappa$ B activity and inflammation, but did not affect type I and III IFNs  
285 production.

286 Consistent with our previous findings (27), IAV infections in COPD pBECs and  
287 experimental COPD led to heightened inflammation and production of inflammatory cytokines

288 but impaired antiviral responses (IFN- $\beta$  and IFN- $\lambda$ ), which were associated with greater viral  
289 replication. Increased inflammation, inflammatory cytokines and activation of NF- $\kappa$ B are well-  
290 known in COPD (24, 44). Here we show that these are the result of reduced induction of A20,  
291 leading to uncontrolled activation of NF- $\kappa$ B and subsequent induction of inflammatory  
292 cytokines. A20 is a pleiotropic protein involved in various ubiquitin-dependent pathways  
293 including NF- $\kappa$ B (16) and mitogen-activated protein (MAP) kinase pathway (45), and has also  
294 been shown to negatively regulate type I IFN inductions (43, 46, 47). Surprisingly inhibition  
295 or ectopic expression of A20 did not affect IFN- $\beta$  production. The precise roles of A20 during  
296 viral infections therefore require further investigation. We could not rule out that other factors  
297 may also contribute to the regulation of A20 expression and of NF- $\kappa$ B activity, including other  
298 un-identified miRNAs, which may also be dys-regulated in COPD.

299         Forced expression of A20 may be a novel therapeutic option that reduces IAV-  
300 mediated inflammation and cytokine storm, particularly from high pathogenic IAVs such as  
301 H5N1, or in COPD where airway inflammation is already persistently heightened.

302         The lack of the induction of A20 protein during IAV infection in COPD was attributed  
303 to increased levels of miR-125a and b. These miRNAs down-regulate A20 expression by  
304 directly binding to its 3'-UTR, leading to constitutive activation of NF- $\kappa$ B (16). We found that  
305 heightened levels of miR-125a/b resulted in increased activation of NF- $\kappa$ B in COPD. Inhibition  
306 of miR-125a or b in both healthy and COPD pBECs and in experimental COPD increased A20  
307 protein levels and reduced NF- $\kappa$ B activation during IAV infection.

308         We also found that miR-125a and b modulated the induction of type I and III antiviral  
309 IFNs. This occurred by the direct targeting of MAVS 3'-UTR, therefore down-regulating the  
310 subsequent induction of IFN- $\beta$  and IFN- $\lambda$ . MAVS is an important adaptor protein on  
311 mitochondria that facilitates the production of IFNs (8), however there was an impaired  
312 induction of MAVS by IAV infections in COPD pBECs and in experimental COPD. Inhibition

313 of miR-125a and/or b increased the levels of MAVS and antiviral IFNs, which lead to reduced  
314 virus replication both *in vivo* and *in vivo*. Interestingly antagomiRs against miR-125a and/or b  
315 (either alone or in combination) in experimental COPD, partially reduced the release of  
316 inflammatory cytokines, and substantially suppressed virus replication. This may indicate that  
317 miR-125a and b may preferentially target MAVS over A20 during IAV infection in COPD,  
318 although such binding preferences of miRNAs have not been widely investigated. Furthermore,  
319 as MAVS is transcriptionally driven by IFN-sensitive response element (ISRE) as part of the  
320 IFN-stimulated genes (48), and miR-125a/b have been reported to be induced by NF- $\kappa$ B (49),  
321 it is possible that reduced MAVS partly attributed to impaired IFNs in COPD, and with  
322 enhanced expression of miR-125a/b (NF- $\kappa$ B-inducible) this then leads to continuous cycle of  
323 exaggerated inflammation and impaired antiviral immunity in COPD.

324         Although miR-125a/b appears to be NF- $\kappa$ B-inducible, the exact molecular  
325 mechanisms of enhanced miR-125a/b expression in COPD require further investigation. In  
326 colorectal cancer tissues the levels of miR-125a have been shown to be reduced, which is  
327 associated with hyper-methylation at the CpG island within the promoter region of miR-125a  
328 (50). Similarly in breast cancer cell line reduced miR-125a has also been shown to be associated  
329 with tri-methylation at H3K9 and H3K27 at the promoter region of miR-125a (51). It is  
330 therefore possible that the methylation status of miR-125a/b promoter site is altered in COPD,  
331 leading to increased expression of miR-125a/b. Nevertheless, our data also demonstrate that  
332 specific inhibition of miR-125a/b may be novel therapeutic options against IAV infections and  
333 for those whom are most vulnerable.

334         Cigarette smoke is the major risk factor for COPD. Acute exposure results in  
335 oxidative stress and NF- $\kappa$ B activation (52-54). However the effects we have observed in  
336 COPD appear to be independent of acute exposure to cigarette smoking, as the pBECs obtained  
337 from subjects with COPD were all abstinent from smoking for at least 10 years. It is likely that

338 chronic exposure progressively leads to persistent induction of miR-125a and b and NF- $\kappa$ B  
339 activation (55, 56), that then reduces the induction of A20 and MAVS in COPD.

340 Collectively, our results demonstrate that A20 regulates NF- $\kappa$ B activation and  
341 subsequently the production of inflammatory cytokines but not antiviral IFNs. COPD pBECs  
342 and mice with experimental COPD responded to IAV infection with an exaggerated  
343 inflammatory but impaired antiviral responses. Increased levels of miR-125a and b by IAV and  
344 in COPD suppressed protein inductions of A20 and MAVS, leading to heightened airway  
345 inflammation and reduced IFN production. Inhibition of miR-125a and b reduced the induction  
346 of inflammatory cytokines and enhanced antiviral responses to IAV infection in both healthy  
347 and COPD states. This study therefore identifies a novel potential therapeutic target for IAV  
348 infection in general and in COPD.

349

## 350 **Materials and Methods**

### 351 **Ex vivo:**

352 COPD patients (10) and healthy non-smoking (10) and smoking (5) controls were recruited  
353 and their characteristics are shown in Table 1. Subject recruitment, viruses, cell culture and  
354 viral infection, A20 plasmid, siRNA, and miR-125a and b antagomiR/mimetic treatment,  
355 cloning and mutagenesis of miR-125a and b binding sites in the MAVS 3'-UTR, reporter  
356 assays, immunoblotting, cytometric bead array, immunoprecipitation, miR extraction and  
357 analysis, and statistical tests were performed as previously described and/or as in the online  
358 supplement (27, 31, 57, 58).

359

### 360 **In vivo:**

361 Experimental COPD and influenza infection were induced, miR-125a and b was inhibited using  
362 specific antagomiRs, histopathology, immunohistochemistry, immunoblotting and cytometric

363 bead array and data analyses were performed as previously described and/or as in online  
364 supplement (33, 35, 39, 59-67).

365

### 366 **Study Approvals**

367 All procedures were approved by The University of Newcastle Human and Animal Ethics  
368 Committees.

369

### 370 **Author contributions**

371 A. C-Y. H. conceived and designed the study. A. C-Y. H. and K. P. performed all *in vitro*  
372 experiments. K. D., T-J. H., and P. M. N. performed all *in vivo* experiments. All authors  
373 participated in the completion of the manuscript.

374

375 **Acknowledgements:** This study is funded by National Health and Medical Research Council  
376 of Australia (Grant no. 1045762), and University of Newcastle (Grant no.1300661). The  
377 authors thank Kristy Wheeldon and Nathalie Kiaos for technical assistance with *in vivo*  
378 protocols.

379

### 380 **References**

381 1. Hallstrand TS, Hackett TL, Altemeier WA, Matute-Bello G, Hansbro PM, and Knight  
382 DA. Airway epithelial regulation of pulmonary immune homeostasis and inflammation. *Clin*  
383 *Immunol.* 2014;151(1):1-15.

384 2. Hsu AC, See HV, and Wark PA. Innate immunity to influenza in chronic airways  
385 diseases. *Respirology.* 2012.

- 386 3. Chaouat A, Savale L, Chouaid C, Tu L, Sztrymf B, Canuet M, Maitre B, Housset B,  
387 Brandt C, Le Corvoisier P, et al. Role for interleukin-6 in COPD-related pulmonary  
388 hypertension. *Chest*. 2009;136(3):678-87.
- 389 4. Meylan E, Burns K, Hofmann K, Blancheteau V, Martinon F, Kelliher M, and Tschopp  
390 J. RIP1 is an essential mediator of Toll-like receptor 3-induced NF-kappa B activation. *Nature*  
391 *immunology*. 2004;5(5):503-7.
- 392 5. Monks BG, Martell BA, Buras JA, and Fenton MJ. An upstream protein interacts with  
393 a distinct protein that binds to the cap site of the human interleukin 1 beta gene. *Molecular*  
394 *immunology*. 1994;31(2):139-51.
- 395 6. Tate MD, Ioannidis LJ, Croker B, Brown LE, Brooks AG, and Reading PC. The role  
396 of neutrophils during mild and severe influenza virus infections of mice. *PLoS ONE*.  
397 2011;6(3):e17618.
- 398 7. Hashimoto Y, Moki T, Takizawa T, Shiratsuchi A, and Nakanishi Y. Evidence for  
399 phagocytosis of influenza virus-infected, apoptotic cells by neutrophils and macrophages in  
400 mice. *J Immunol*. 2007;178(4):2448-57.
- 401 8. Seth RB, Sun L, Ea CK, and Chen ZJ. Identification and characterization of MAVS, a  
402 mitochondrial antiviral signaling protein that activates NF-kappaB and IRF 3. *Cell*.  
403 2005;122(5):669-82.
- 404 9. Hsu AC, Parsons K, Barr I, Lowther S, Middleton D, Hansbro P, and Wark P. Critical  
405 role of type I interferon response in bronchial epithelial cell to influenza infection. *PLoS ONE*.  
406 2012;7(3):e32947.

- 407 10. Verhelst J, Parthoens E, Schepens B, Fiers W, and Saelens X. Interferon-inducible  
408 protein Mx1 inhibits influenza virus by interfering with functional viral ribonucleoprotein  
409 complex assembly. *Journal of virology*. 2012;86(24):13445-55.
- 410 11. Heyninck K, De Valck D, Vanden Berghe W, Van Criekinge W, Contreras R, Fiers W,  
411 Haegeman G, and Beyaert R. The zinc finger protein A20 inhibits TNF-induced NF-kappaB-  
412 dependent gene expression by interfering with an RIP- or TRAF2-mediated transactivation  
413 signal and directly binds to a novel NF-kappaB-inhibiting protein ABIN. *J Cell Biol*.  
414 1999;145(7):1471-82.
- 415 12. Heyninck K, and Beyaert R. The cytokine-inducible zinc finger protein A20 inhibits  
416 IL-1-induced NF-kappaB activation at the level of TRAF6. *FEBS letters*. 1999;442(2-3):147-  
417 50.
- 418 13. Grey ST, Arvelo MB, Hasenkamp W, Bach FH, and Ferran C. A20 inhibits cytokine-  
419 induced apoptosis and nuclear factor kappaB-dependent gene activation in islets. *The Journal*  
420 *of experimental medicine*. 1999;190(8):1135-46.
- 421 14. Ferran C, Stroka DM, Badrichani AZ, Cooper JT, Wrighton CJ, Soares M, Grey ST,  
422 and Bach FH. A20 inhibits NF-kappaB activation in endothelial cells without sensitizing to  
423 tumor necrosis factor-mediated apoptosis. *Blood*. 1998;91(7):2249-58.
- 424 15. Foster PS, Plank M, Collison A, Tay HL, Kaiko GE, Li J, Johnston SL, Hansbro PM,  
425 Kumar RK, Yang M, et al. The emerging role of microRNAs in regulating immune and  
426 inflammatory responses in the lung. *Immunological reviews*. 2013;253(1):198-215.
- 427 16. Kim SW, Ramasamy K, Bouamar H, Lin AP, Jiang D, and Aguiar RC. MicroRNAs  
428 miR-125a and miR-125b constitutively activate the NF-kappaB pathway by targeting the tumor

429 necrosis factor alpha-induced protein 3 (TNFAIP3, A20). *Proceedings of the National*  
430 *Academy of Sciences of the United States of America*. 2012;109(20):7865-70.

431 17. WHO. Chronic Obstructive Pulmonary Disease (COPD). *Fact Sheet No 315*.  
432 2012;accessed November 2012(

433 18. Lopez AD, Mathers CD, Ezzati M, Jamison DT, and Murray CJ. Global and regional  
434 burden of disease and risk factors, 2001: systematic analysis of population health data. *Lancet*.  
435 2006;367(9524):1747-57.

436 19. Hurst JR, Vestbo J, Anzueto A, Locantore N, Mallerova H, Tal-Singer R, Miller B,  
437 Lomas DA, Agusti A, MacNee W, et al. Susceptibility to Exacerbation in Chronic Obstructive  
438 Pulmonary Disease. *New England Journal of Medicine*. 2010;363(12):1128-38.

439 20. Soler-Cataluna JJ, Martinez-Garcia MA, Roman Sanchez P, Salcedo E, Navarro M, and  
440 Ochando R. Severe acute exacerbations and mortality in patients with chronic obstructive  
441 pulmonary disease. *Thorax*. 2005;60(11):925-31.

442 21. Seemungal T, Harper-Owen R, Bhowmik A, Moric I, Sanderson G, Message S,  
443 Maccallum P, Meade TW, Jeffries DJ, Johnston SL, et al. Respiratory viruses, symptoms, and  
444 inflammatory markers in acute exacerbations and stable chronic obstructive pulmonary  
445 disease. *American journal of respiratory and critical care medicine*. 2001;164(9):1618-23.

446 22. Nath KD, Burel JG, Shankar V, Pritchard AL, Towers M, Looke D, Davies JM, and  
447 Upham JW. Clinical factors associated with the humoral immune response to influenza  
448 vaccination in chronic obstructive pulmonary disease. *Int J Chron Obstruct Pulmon Dis*.  
449 2014;9(51-6).

- 450 23. Hurt AC, Hardie K, Wilson NJ, Deng YM, Osbourn M, Gehrig N, and Kelso A.  
451 Community transmission of oseltamivir-resistant A(H1N1)pdm09 influenza. *The New England*  
452 *journal of medicine*. 2011;365(26):2541-2.
- 453 24. Di Stefano A, Caramori G, Oates T, Capelli A, Lusuardi M, Gnemmi I, Ioli F, Chung  
454 KF, Donner CF, Barnes PJ, et al. Increased expression of nuclear factor-kappaB in bronchial  
455 biopsies from smokers and patients with COPD. *Eur Respir J*. 2002;20(3):556-63.
- 456 25. Hsu AC, Barr I, Hansbro PM, and Wark PA. Human influenza is more effective than  
457 avian influenza at antiviral suppression in airway cells. *Am J Respir Cell Mol Biol*.  
458 2011;44(6):906-13.
- 459 26. Chan MC, Cheung CY, Chui WH, Tsao SW, Nicholls JM, Chan YO, Chan RW, Long  
460 HT, Poon LL, Guan Y, et al. Proinflammatory cytokine responses induced by influenza A  
461 (H5N1) viruses in primary human alveolar and bronchial epithelial cells. *Respiratory research*.  
462 2005;6(135).
- 463 27. Hsu A, Starkey MR, Hanish I, Parsons K, Haw TJ, Howland LJ, Barr I, Mahony JB,  
464 Foster PS, Knight DA, et al. Targeting PI3K-p110alpha Suppresses Influenza Virus Infection  
465 in Chronic Obstructive Pulmonary Disease. *American journal of respiratory and critical care*  
466 *medicine*. 2015;191(9):1012-23.
- 467 28. Beckett EL, Stevens RL, Jarnicki AG, Kim RY, Hanish I, Hansbro NG, Deane A, Keely  
468 S, Horvat JC, Yang M, et al. A new short-term mouse model of chronic obstructive pulmonary  
469 disease identifies a role for mast cell tryptase in pathogenesis. *J Allergy Clin Immunol*.  
470 2013;131(3):752-62.
- 471 29. Hsu AC, Parsons K, Moheimani F, Knight DA, Hansbro PM, Fujita T, and Wark PA.  
472 Impaired Antiviral Stress Granule and IFN-beta Enhanceosome Formation Enhances

473 Susceptibility to Influenza Infection in Chronic Obstructive Pulmonary Disease Epithelium.  
474 *American journal of respiratory cell and molecular biology*. 2016;55(1):117-27.

475 30. Tay HL, Kaiko GE, Plank M, Li J, Maltby S, Essilfie AT, Jarnicki A, Yang M, Mattes  
476 J, Hansbro PM, et al. Antagonism of miR-328 increases the antimicrobial function of  
477 macrophages and neutrophils and rapid clearance of non-typeable *Haemophilus influenzae*  
478 (NTHi) from infected lung. *PLoS pathogens*. 2015;11(4):e1004549.

479 31. Conickx G, Mestdagh P, Cobos FA, Verhamme FM, Maes T, Vanaudenaerde BM, Seys  
480 LJM, Lahousse L, Kim RY, Hsu AC, et al. MicroRNA profiling reveals a role for microRNA-  
481 218-5p in the pathogenesis of chronic obstructive pulmonary disease. *American journal of*  
482 *respiratory and critical care medicine*. 2016;In Press(

483 32. Fricker M, Deane A, and Hansbro PM. Animal models of chronic obstructive  
484 pulmonary disease. *Expert Opin Drug Discov*. 2014;9(6):629-45.

485 33. Franklin BS, Bossaller L, De Nardo D, Ratter JM, Stutz A, Engels G, Brenker C,  
486 Nordhoff M, Mirandola SR, Al-Amoudi A, et al. The adaptor ASC has extracellular and  
487 'prionoid' activities that propagate inflammation. *Nature immunology*. 2014;15(8):727-37.

488 34. Hansbro PM, Hamilton MJ, Fricker M, Gellatly SL, Jarnicki AG, Zheng D, Frei SM,  
489 Wong GW, Hamadi S, Zhou S, et al. Importance of mast cell Prss31/transmembrane  
490 tryptase/tryptase-gamma in lung function and experimental chronic obstructive pulmonary  
491 disease and colitis. *The Journal of biological chemistry*. 2014;289(26):18214-27.

492 35. Haw TJ, Starkey MR, Nair PM, Pavlidis S, Liu G, Nguyen DH, Hsu AC, Hanish I, Kim  
493 RY, Collison AM, et al. A pathogenic role for tumor necrosis factor-related apoptosis-inducing  
494 ligand in chronic obstructive pulmonary disease. *Mucosal Immunol*. 2015;Advance online  
495 publication. 10.1038/mi.2015.111(

- 496 36. Hsu AC, Parsons K, Hansbro PM, and Wark P. *Federation of Immunological Societies*  
497 *of Asia-Oceania*. Singapore; 2015.
- 498 37. Hussain S, Sangtian S, Anderson SM, Snyder RJ, Marshburn JD, Rice AB, Bonner JC,  
499 and Garantziotis S. Inflammasome activation in airway epithelial cells after multi-walled  
500 carbon nanotube exposure mediates a profibrotic response in lung fibroblasts. *Part Fibre*  
501 *Toxicol*. 2014;11(28).
- 502 38. Higham A, Lea S, Ray D, and Singh D. Corticosteroid effects on COPD alveolar  
503 macrophages: dependency on cell culture methodology. *J Immunol Methods*. 2014;405(144-  
504 53.
- 505 39. Liu G, Cooley MA, Jarnicki AG, Hsu ACY, Nair PM, Haw TJ, Fricker M, Gellatly SL,  
506 Kim RY, Inman MD, et al. Fibulin-1 regulates the pathogenesis of tissue remodeling in  
507 respiratory diseases. *JCI Insight*. 2016;1(9):e86380(
- 508 40. Asher MI, Montefort S, Björkstén B, Lai CK, Strachan DP, Weiland SK, Williams H,  
509 and ISAAC Phase Three Study Group. Worldwide time trends in the prevalence of symptoms  
510 of asthma, allergic rhinoconjunctivitis, and eczema in childhood: ISAAC Phases One and  
511 Three repeat multicountry cross sectional surveys. *Lancet*. 2006;368(9537):733-43.
- 512 41. Kanner RE, Anthonisen NR, Connett JE, and Lung Health Study Research G. Lower  
513 respiratory illnesses promote FEV(1) decline in current smokers but not ex-smokers with mild  
514 chronic obstructive pulmonary disease: results from the lung health study. *Am J Respir Crit*  
515 *Care Med*. 2001;164(3):358-64.
- 516 42. Seemungal TA, Donaldson GC, Paul EA, Bestall JC, Jeffries DJ, and Wedzicha JA.  
517 Effect of exacerbation on quality of life in patients with chronic obstructive pulmonary disease.  
518 *Am J Respir Crit Care Med*. 1998;157(5 Pt 1):1418-22.

- 519 43. Wang YY, Li L, Han KJ, Zhai Z, and Shu HB. A20 is a potent inhibitor of TLR3- and  
520 Sendai virus-induced activation of NF-kappaB and ISRE and IFN-beta promoter. *FEBS letters*.  
521 2004;576(1-2):86-90.
- 522 44. Barnes PJ. The cytokine network in asthma and chronic obstructive pulmonary disease.  
523 *J Clin Invest*. 2008;118(11):3546-56.
- 524 45. Jung SM, Lee JH, Park J, Oh YS, Lee SK, Park JS, Lee YS, Kim JH, Lee JY, Bae YS,  
525 et al. Smad6 inhibits non-canonical TGF-beta1 signalling by recruiting the deubiquitinase A20  
526 to TRAF6. *Nat Commun*. 2013;4(2562).
- 527 46. Saitoh T, Yamamoto M, Miyagishi M, Taira K, Nakanishi M, Fujita T, Akira S,  
528 Yamamoto N, and Yamaoka S. A20 is a negative regulator of IFN regulatory factor 3 signaling.  
529 *J Immunol*. 2005;174(3):1507-12.
- 530 47. Maelfait J, Roose K, Bogaert P, Sze M, Saelens X, Pasparakis M, Carpentier I, van Loo  
531 G, and Beyaert R. A20 (Tnfaip3) deficiency in myeloid cells protects against influenza A virus  
532 infection. *PLoS pathogens*. 2012;8(3):e1002570.
- 533 48. Rusinova I, Forster S, Yu S, Kannan A, Masse M, Cumming H, Chapman R, and  
534 Hertzog PJ. Interferome v2.0: an updated database of annotated interferon-regulated genes.  
535 *Nucleic acids research*. 2013;41(Database issue):D1040-6.
- 536 49. Lee HM, Kim TS, and Jo EK. MiR-146 and miR-125 in the regulation of innate  
537 immunity and inflammation. *BMB Rep*. 2016;49(6):311-8.
- 538 50. Chen H, and Xu Z. Hypermethylation-Associated Silencing of miR-125a and miR-  
539 125b: A Potential Marker in Colorectal Cancer. *Dis Markers*. 2015;2015(345080).

- 540 51. Cisneros-Soberanis F, Andonegui MA, and Herrera LA. miR-125b-1 is repressed by  
541 histone modifications in breast cancer cell lines. *Springerplus*. 2016;5(1):959.
- 542 52. Kirkham PA, and Barnes PJ. Oxidative stress in COPD. *Chest*. 2013;144(1):266-73.
- 543 53. Fischer BM, Pavlisko E, and Voynow JA. Pathogenic triad in COPD: oxidative stress,  
544 protease-antiprotease imbalance, and inflammation. *Int J Chron Obstruct Pulmon Dis*.  
545 2011;6(4):13-21.
- 546 54. Kratsovnik E, Bromberg Y, Sperling O, and Zoref-Shani E. Oxidative stress activates  
547 transcription factor NF-kB-mediated protective signaling in primary rat neuronal cultures. *J*  
548 *Mol Neurosci*. 2005;26(1):27-32.
- 549 55. Tan G, Niu J, Shi Y, Ouyang H, and Wu ZH. NF-kappaB-dependent microRNA-125b  
550 up-regulation promotes cell survival by targeting p38alpha upon ultraviolet radiation. *The*  
551 *Journal of biological chemistry*. 2012;287(39):33036-47.
- 552 56. Werner SL, Kearns JD, Zadorozhnaya V, Lynch C, O'Dea E, Boldin MP, Ma A,  
553 Baltimore D, and Hoffmann A. Encoding NF-kappaB temporal control in response to TNF:  
554 distinct roles for the negative regulators IkappaBalpha and A20. *Genes & development*.  
555 2008;22(15):2093-101.
- 556 57. Gomez FP, and Rodriguez-Roisin R. Global Initiative for Chronic Obstructive Lung  
557 Disease (GOLD) guidelines for chronic obstructive pulmonary disease. *Curr Opin Pulm Med*.  
558 2002;8(2):81-6.
- 559 58. Hurd SZ. Workshop summary and guidelines: Investigative use of bronchoscopy. *J*  
560 *Allergy Clin Immunol*. 1991;88(5):808-14.

- 561 59. Horvat JC, Starkey MR, Kim RY, Beagley KW, Preston JA, Gibson PG, Foster PS, and  
562 Hansbro PM. Chlamydial respiratory infection during allergen sensitization drives neutrophilic  
563 allergic airways disease. *J Immunol.* 2010;184(8):4159-69.
- 564 60. Thorburn AN, Foster PS, Gibson PG, and Hansbro PM. Components of *Streptococcus*  
565 *pneumoniae* suppress allergic airways disease and NKT cells by inducing regulatory T cells. *J*  
566 *Immunol.* 2012;188(9):4611-20.
- 567 61. Essilfie AT, Horvat JC, Kim RY, Mayall JR, Pinkerton JW, Beckett EL, Starkey MR,  
568 Simpson JL, Foster PS, Gibson PG, et al. Macrolide therapy suppresses key features of  
569 experimental steroid-sensitive and steroid-insensitive asthma. *Thorax.* 2015;70(5):458-67.
- 570 62. Plank MW, Maltby S, Tay HL, Stewart J, Eyers F, Hansbro PM, and Foster PS.  
571 MicroRNA Expression Is Altered in an Ovalbumin-Induced Asthma Model and Targeting  
572 miR-155 with Antagomirs Reveals Cellular Specificity. *PLoS One.* 2015;10(12):e0144810.
- 573 63. Preston JA, Essilfie AT, Horvat JC, Wade MA, Beagley KW, Gibson PG, Foster PS,  
574 and Hansbro PM. Inhibition of allergic airways disease by immunomodulatory therapy with  
575 whole killed *Streptococcus pneumoniae*. *Vaccine.* 2007;25(48):8154-62.
- 576 64. Asquith KL, Horvat JC, Kaiko GE, Carey AJ, Beagley KW, Hansbro PM, and Foster  
577 PS. Interleukin-13 promotes susceptibility to chlamydial infection of the respiratory and genital  
578 tracts. *PLoS pathogens.* 2011;7(5):e1001339.
- 579 65. Starkey MR, Essilfie AT, Horvat JC, Kim RY, Nguyen DH, Beagley KW, Mattes J,  
580 Foster PS, and Hansbro PM. Constitutive production of IL-13 promotes early-life *Chlamydia*  
581 respiratory infection and allergic airway disease. *Mucosal Immunol.* 2013;6(3):569-79.
- 582 66. Starkey MR, Nguyen DH, Essilfie AT, Kim RY, Hatchwell LM, Collison AM, Yagita  
583 H, Foster PS, Horvat JC, Mattes J, et al. Tumor necrosis factor-related apoptosis-inducing

584 ligand translates neonatal respiratory infection into chronic lung disease. *Mucosal Immunol.*  
585 2014;7(3):478-88.

586 67. Kim RY, Horvat JC, Pinkerton JW, Starkey MR, Essilfie AT, Mayall JR, Nair PM,  
587 Hansbro NG, Jones B, Haw TJ, et al. MicroRNA-21 drives severe, steroid-insensitive  
588 experimental asthma by amplifying PI3K-mediated suppression of HDAC2. *J Allergy Clin*  
589 *Immunol.* Accepted 30 Apr 2016(

590

591 **Table 1. Subject characteristics**

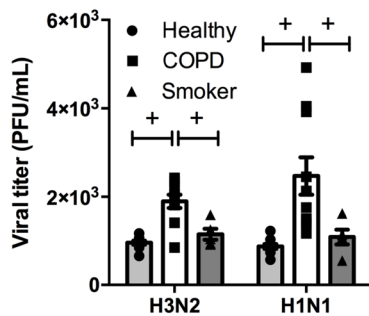
	<b>Healthy</b>	<b>COPD</b>	<b>Smoker</b>	<b>P – value</b>
<b>Number</b>	15	15	5	NA
<b>Sex (Male:Female ratio)</b>	1.14	1.2	1.5	p = 0.6
<b>Mean Age (SD)</b>	62 (9.9)	68 (4.1)	64.33 (12.82)	p = 0.06
<b>Mean FEV<sub>1</sub> (SD) *</b>	105% (13.5)	40% (7.75)	97.66% (12.66)	p < 0.001
<b>FEV<sub>1</sub>/FVC ratio (SD) *</b>	886x (14.50)	40.20 (13.50)	77.80 (12.28)	p < 0.001
<b>Cigarette (Packs/year; SD)</b>	0	53.70 (15.90)	30 (17.32)	p < 0.001
<b>Years abstinent (SD)</b>	0	13.0 (4.64)	0	NA
<b>ICS (percent treated)</b>	0	Seretide (10%) Spiriva (10%) Tiotropium (10%) Spiriva/Salbutamol (10%) Seretide/Tiotropium (20%) Seretide/Tiotropium/Ventolin (20%) Seretide/Spiriva/Ventolin (20%)	0	NA

592 \*FEV<sub>1</sub> and FEV<sub>1</sub>/FVC ratios are % predicted values. FEV<sub>1</sub> is the forced expiratory volume in  
 593 1s expressed as a percentage of the predicated value. FVC is forced vital capacity. The  
 594 statistical analysis used was ANOVA for multiple groups. NA = Not applicable.

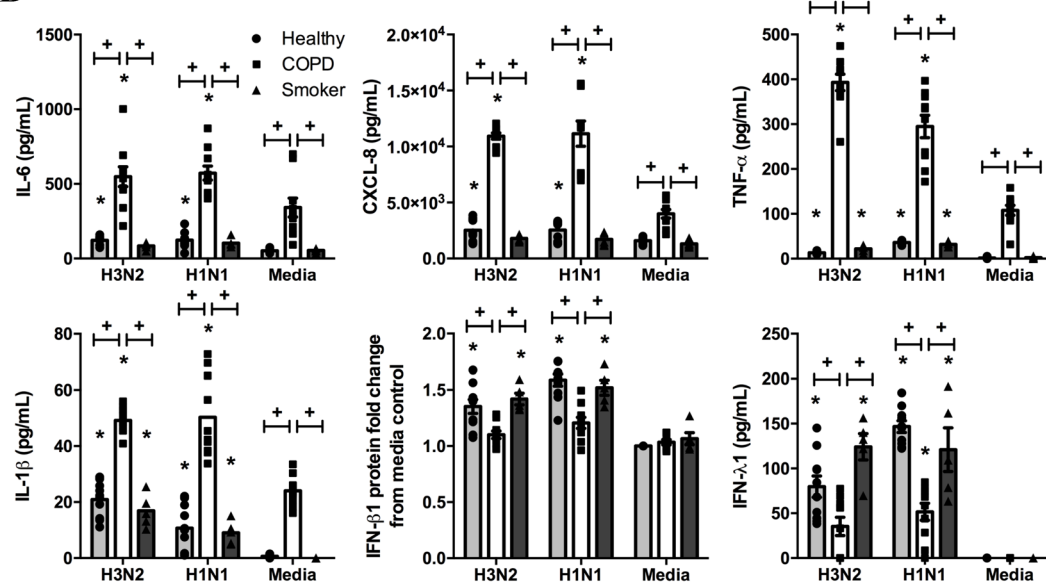
595

**Figure 1**

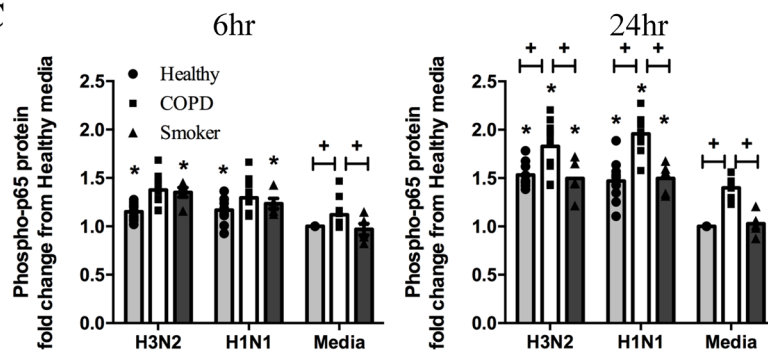
**A**



**B**



**C**

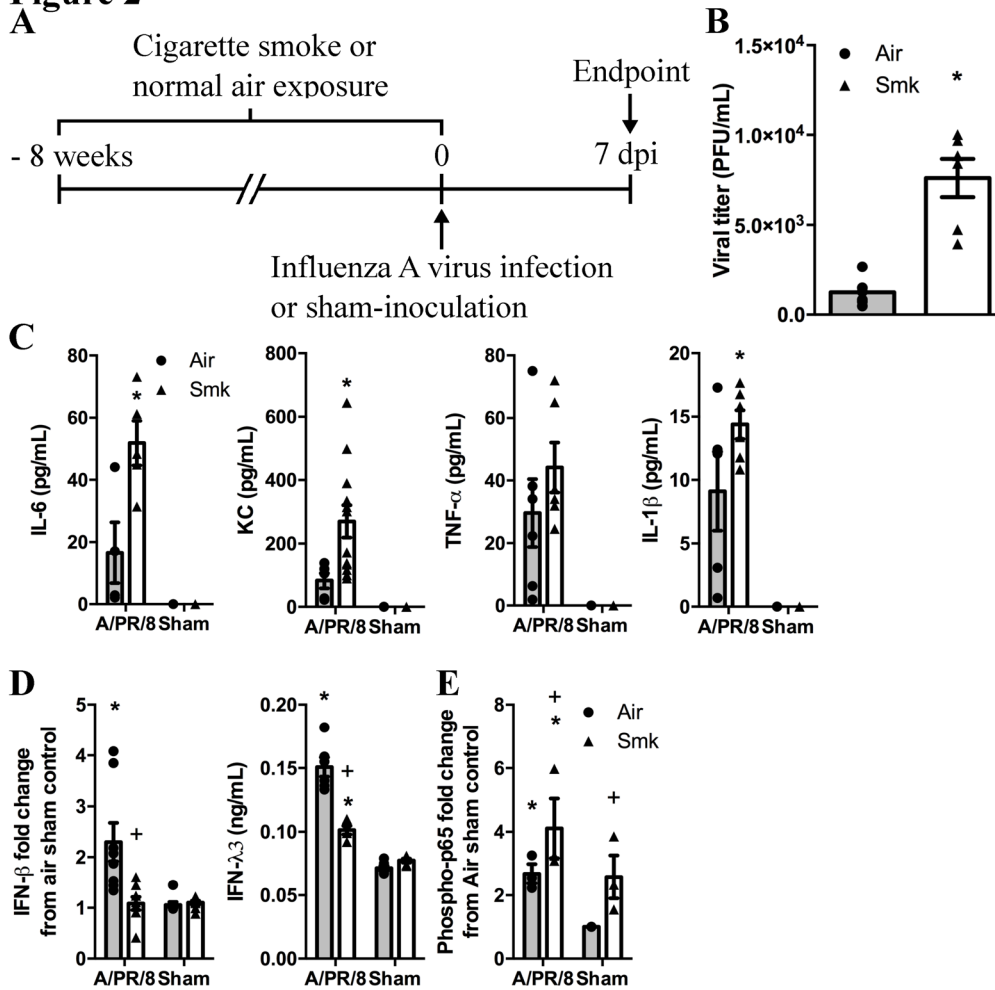


597

598 **Fig. 1.** IAV infection is more severe and results in exaggerated inflammatory but impaired  
 599 antiviral responses in pBECs from patients with COPD. pBECs from healthy controls, COPD  
 600 patients and healthy smokers were infected with human IAV H3N2 or H1N1, and (A) virus  
 601 replication was measured at 24hr. (B) Pro-inflammatory cytokines/chemokines IL-6, CXCL-  
 602 8, TNF- $\alpha$ , and IL-1 $\beta$ , and antiviral cytokines IFN- $\beta$  and IFN- $\lambda$ 1 were measured in culture

603 supernatants at 24hr. (C) Phospho-p65 was assessed at 6hr and 24hr, densitometry results (from  
604 Supplementary Fig. S1A, representative immunoblot) were calculated as phospho-  
605 p65:GAPDH ratios, and expressed as fold change from healthy media control. Data are mean  
606  $\pm$  SEM,  $n = 15$  (healthy controls and COPD patients) or 5 (healthy smokers). \* $P \leq 0.05$  versus  
607 respective un-infected media control, +  $P \leq 0.05$  versus infected or un-infected healthy controls.  
608 Statistical differences were determined with one-way ANOVA followed by Bonferroni post-  
609 test.  
610

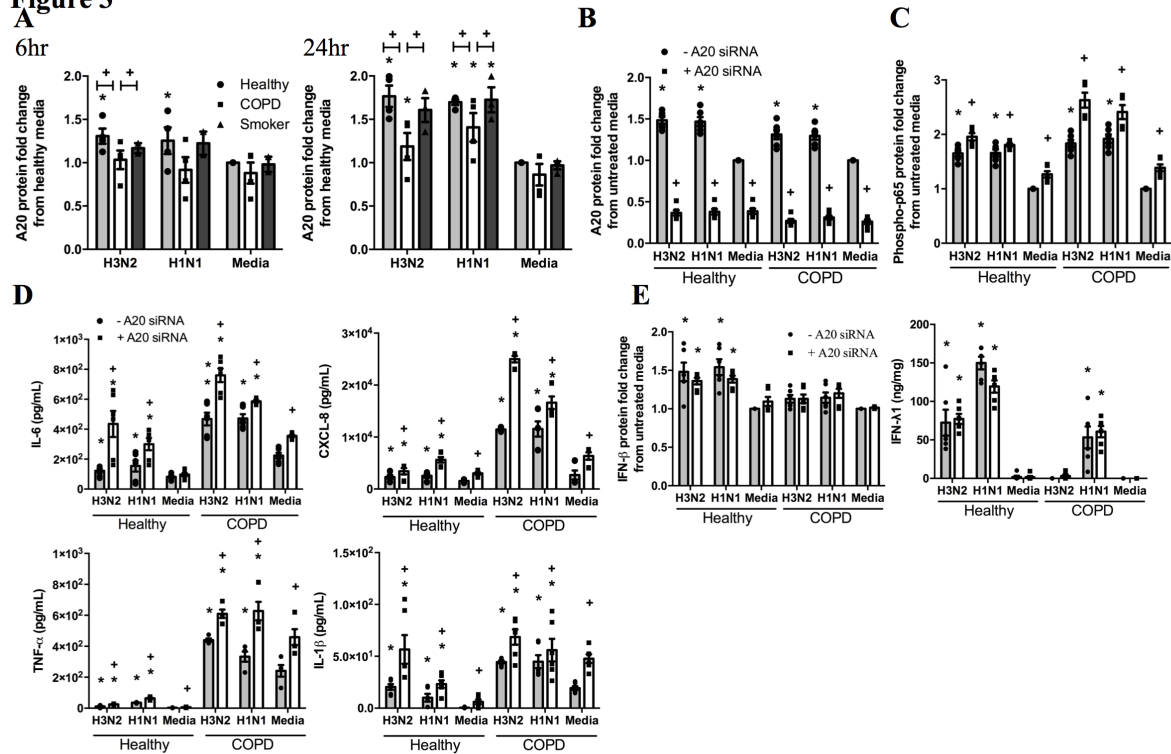
**Figure 2**



611

612 **Fig. 2.** IAV infection is more severe and results in exaggerated inflammatory and impaired  
613 antiviral responses in experimental COPD. (A) BALB/c mice were exposed to cigarette smoke  
614 (Smk) or normal air (Air) for eight weeks, infected with IAV H1N1 (A/PR/8/34, 8pfu) or media  
615 (Sham) on the last day of smoke exposure and sacrificed 7 days post infection (dpi). (B) Virus  
616 titers were measured in bronchoalveolar lavage fluid. (C) IL-6, KC, TNF- $\alpha$ , and IL-1 $\beta$ , and (D)  
617 IFN- $\beta$  and IFN- $\lambda$ 3 were assessed in lung homogenates. (E) Phospho-p65 protein was  
618 determined in lung homogenates, densitometry results (from Supplementary Fig. S1D,  
619 representative immunoblot) were calculated as phospho-p65 or IFN- $\beta$ : $\beta$ -actin ratios, and  
620 expressed as fold change from Air sham control. Data are mean  $\pm$  SEM,  $n = 6-8$  per group,

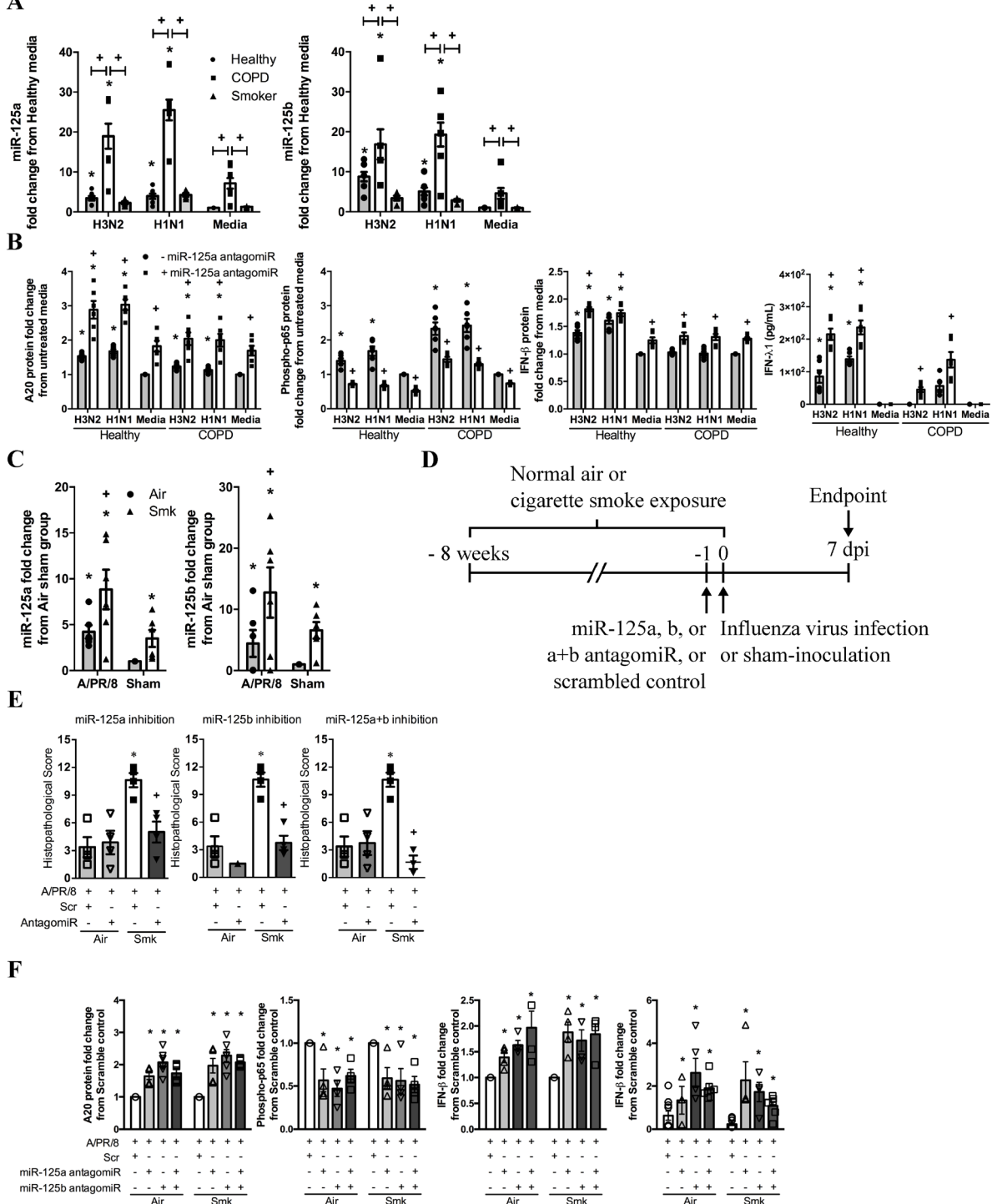
621 \* $P \leq 0.05$  versus Sham control, + $P \leq 0.05$  versus Air control. Statistical differences were  
622 determined with one-way ANOVA followed by Bonferroni post-test.

**Figure 3**

623

624 **Fig. 3.** A20 expression is reduced and it negatively regulates inflammatory but not antiviral  
 625 responses in pBECs from patients with COPD. (A) pBECs were infected with human IAV  
 626 H3N2 or H1N1 and the protein levels of A20 were determined at 6hr and 24hr. Densitometry  
 627 results (from Supplementary Fig. S2A, representative immunoblot) were calculated as A20 or  
 628 phospho-p65:GAPDH ratios, and expressed as fold change from healthy media control. Data  
 629 are mean  $\pm$  SEM,  $n = 15$  per group.  $*P \leq 0.05$  versus respective un-infected media control, +  
 630  $P \leq 0.05$  versus healthy control. A20 expression was inhibited with a specific siRNA, pBECs  
 631 were infected with IAVs and (B) protein levels of A20 and (C) phospho-p65 and of (D)  
 632 cytokines/chemokines IL-6, CXCL-8, TNF- $\alpha$ , and IL-1 $\beta$ , and antiviral (E) IFN- $\beta$  and IFN- $\lambda$ 1  
 633 were measured 24hr later. Densitometric ratios (from Supplementary Fig. S2C, representative  
 634 immunoblot) were expressed as fold change from un-treated media control. Data are mean  $\pm$   
 635 SEM,  $n = 3$  per group.  $*P \leq 0.05$  versus un-treated, un-infected media control, + $P \leq 0.05$  versus  
 636 un-treated infected or un-infected control. Statistical differences were determined with one-  
 637 way ANOVA followed by Bonferroni post-test.

**Figure 4**



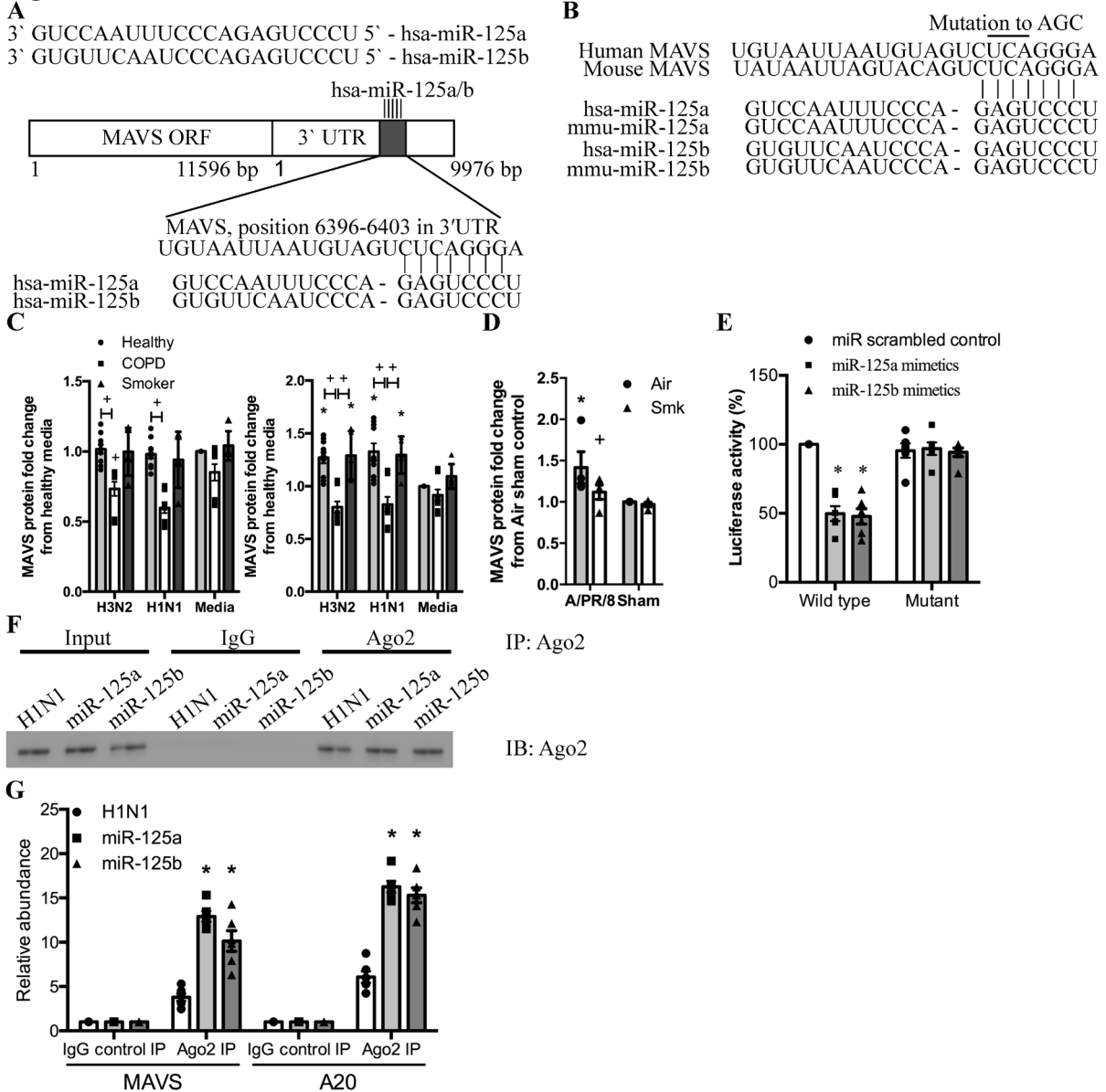
638

639 **Fig. 4.** IAV infection increases the levels of miR-125 and b that suppress the production of  
 640 A20, increase inflammatory and reduce antiviral responses in human COPD pBECs and  
 641 experimental COPD. pBECs were infected with human IAV H3N2 or H1N1 and (A) miR-125a

642 and b levels were assessed 24hr. Data are mean  $\pm$  SEM,  $n = 15$  per group,  $*P \leq 0.05$  versus un-  
643 infected media control.  $+P \leq 0.05$  versus healthy or smoker control. (B) pBECs were treated  
644 with miR-125a or b antagomiR, infected, and the levels of A20, phospho-p65, IFN- $\beta$  and IFN-  
645  $\lambda 1$  were assessed. Densitometry results (Supplementary Fig. S3B, representative immunoblot)  
646 were calculated as A20 or phospho-p65:GAPDH ratios and expressed as fold change from un-  
647 treated, un-infected control. Data are mean  $\pm$  SEM,  $n = 3$  per group,  $*P \leq 0.05$  versus un-treated,  
648 un-infected media control,  $+P \leq 0.05$  versus un-treated infected or un-infected group. (C)  
649 BALB/c mice were exposed to cigarette smoke (Smk) or normal air (Air) for eight weeks,  
650 inoculated with IAV H1N1 (A/PR/8/34, 8pfu) or media (Sham) on the last day of smoke  
651 exposure, sacrificed 7 days post infection (dpi) and the levels of miR-125a and b were  
652 measured. Data are mean  $\pm$  SEM,  $n = 6-8$  per group,  $*P \leq 0.05$  versus Sham group,  $+P \leq 0.05$   
653 versus Air infected or un-infected group. (D) In other groups on the last day of smoke exposure  
654 mice were treated with miR-125a or b antagomiR alone or in combination, infected with IAV,  
655 and (E) airway histological scores were assessed. Data are mean  $\pm$  SEM,  $n = 6-8$  per group,  
656  $*P \leq 0.05$  versus infected and scrambled treated Air controls,  $+P \leq 0.05$  versus infected and  
657 scramble-treated Smk group. (F) The protein levels of A20, phospho-p65, and IFN- $\beta$  in lung  
658 homogenates were also measured. Densitometry results (Supplementary Fig. S4D) were  
659 calculated as A20 or phospho-p65: $\beta$ -actin ratios and expressed as fold change from un-treated,  
660 un-infected control. Data are mean  $\pm$  SEM,  $n = 6-8$  per group,  $*P \leq 0.05$  versus infected  
661 scrambled-treated Air group,  $+P \leq 0.05$  versus infected scrambled Smk group. Statistical  
662 differences were determined with one-way ANOVA followed by Bonferroni post-test.

663

**Figure 5**

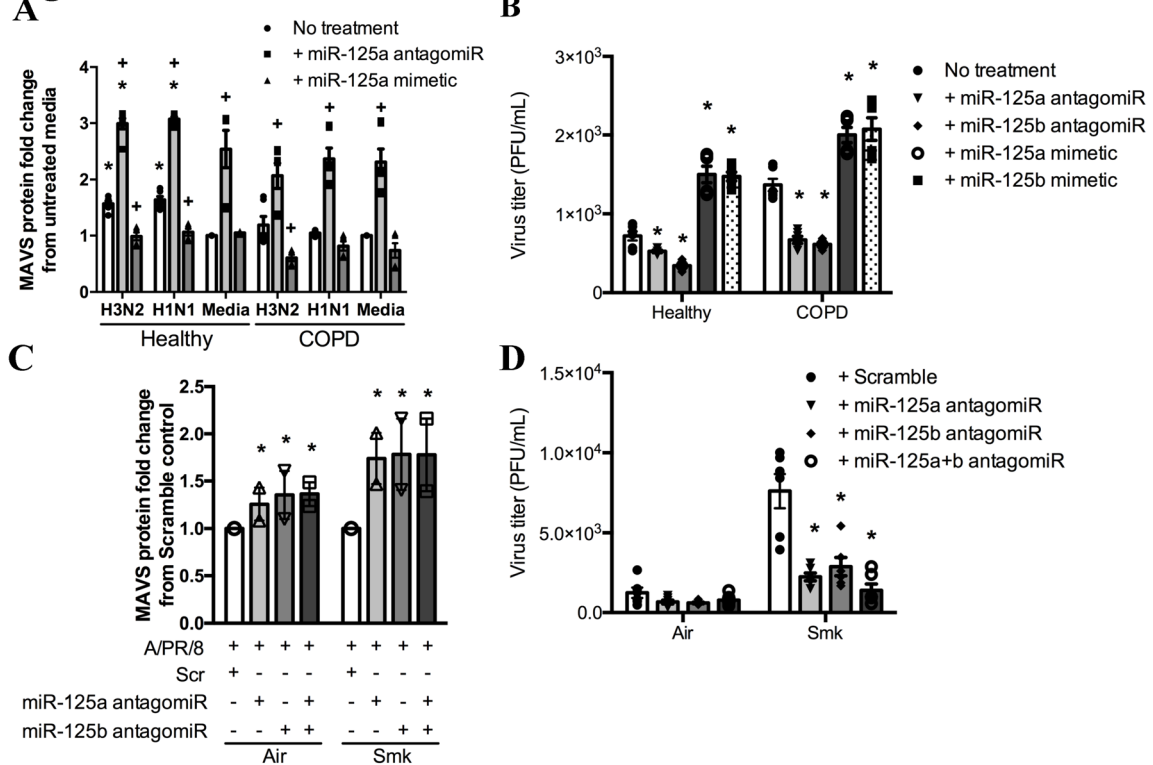


664

665 **Fig. 5.** miR-125a and b target a functional binding site of the 3'-UTR of the mRNA of MAVS  
 666 to suppress its expression. (A) Representation of *MAVS* gene structure and location of miR-  
 667 125a and b binding site. (B) The binding site on 3'-UTR of *MAVS* is 100% conserved between  
 668 human and mouse *MAVS*. (C) pBECs were infected with H3N2 or H1N1 and MAVS protein  
 669 was detected at 6hr and 24hr. Densitometry results (Supplementary Fig. S5A, representative  
 670 immunoblot) were calculated as MAVS:GAPDH ratios and expressed as fold change from un-  
 671 treated, un-infected controls. Data are mean  $\pm$  SEM,  $n = 15$  per group,  $*P \leq 0.05$  versus un-  
 672 infected healthy or smoker controls,  $+P \leq 0.05$  versus infected or un-infected healthy controls.

673 (D) BALB/c mice were exposed to cigarette smoke (Smk) or normal air (Air) for eight weeks,  
674 inoculated with IAV H1N1 (A/PR/8/34, 8pfu) or media (Sham) on the last day of smoke  
675 exposure, sacrificed 7 days post inoculation (dpi) and the levels of MAVS protein were  
676 measured in lung homogenates. Densitometry results (Supplementary Fig. S5B, representative  
677 immunoblot) were calculated as MAVS: $\beta$ -actin ratios in mouse, and expressed as fold change  
678 from un-treated, un-infected controls. Data are mean  $\pm$  SEM,  $n = 6$  per group,  $*P \leq 0.05$  versus  
679 Sham treated controls. +  $P \leq 0.05$  versus infected Air controls. (E) The miR-125a and b binding  
680 site on 3'-UTR was cloned into a pMIR luciferase reporter construct and transfected into  
681 HEK293 cells with miR-125a or b mimetics. The luciferase reporter assay was performed to  
682 determine binding Data are mean  $\pm$  SEM,  $n = 3$  per group,  $*P \leq 0.05$  versus miR scrambled  
683 controls. (F) Ago2 was immunoprecipitated from miR-125a or b mimetic-transfected HEK293,  
684 and (G) A20 and MAVS mRNA was detected by qPCR in Ago2-immunoprecipitate. Data are  
685 mean  $\pm$  SEM,  $n = 3$  per group,  $*P \leq 0.05$  versus IgG control IP. Statistical differences were  
686 determined with one-way ANOVA followed by Bonferroni post-test.

**Figure 6**

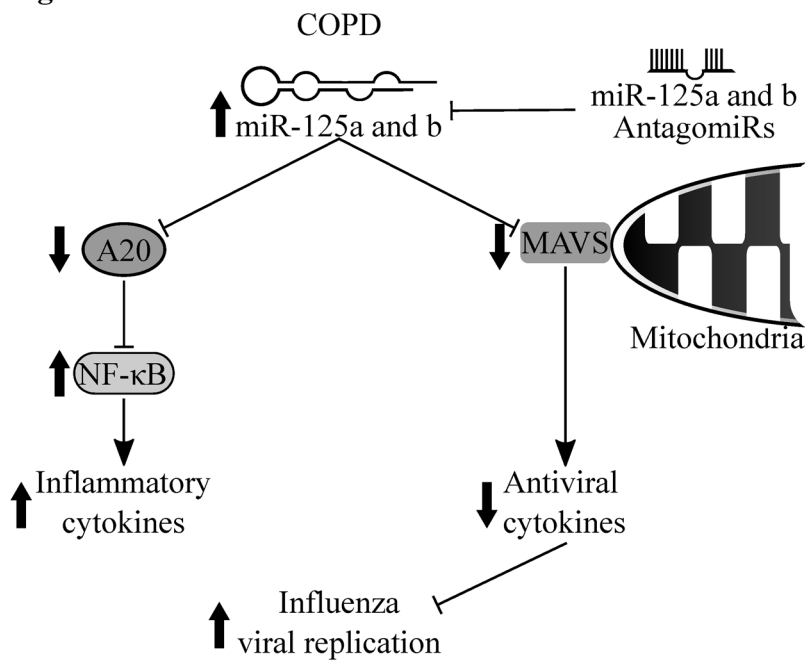


687

688 **Fig. 6.** miR-125a and b suppresses the induction of MAVS and promote virus replication in  
689 human COPD pBECs and experimental COPD. (A) miR-125a and b antagonomiR or mimetics  
690 were added to pBECs before infection with human IAV H3N2 or H1N1 and mitochondrial  
691 antiviral signaling (MAVS) protein were assessed 24hr after infection. Densitometry results  
692 (Supplementary Fig. S6A, representative immunoblot) were calculated as MAVS:GAPDH  
693 ratios and expressed as fold change from un-treated, un-infected controls. Data are mean  $\pm$   
694 SEM,  $n = 3$ ,  $*P \leq 0.05$  versus un-treated, un-infected media controls,  $+P \leq 0.05$  versus un-treated,  
695 infected or un-infected controls. (B) Virus replication was also measured. Data are mean  $\pm$   
696 SEM,  $n = 3$ .  $*P \leq 0.05$  versus un-treated, infected controls. (C) BALB/c mice were exposed to  
697 cigarette smoke (Smk) or normal air (Air) for eight weeks, treated with mir125a and/or b  
698 antagonomiR, infected with IAV H1N1 (A/PR/8/34, 8pfu) or media (Sham) on the last day of  
699 smoke exposure, sacrificed 7 days post inoculation (dpi) and MAVS protein was measured.  
700 Densitometry results (Supplementary Fig. S6C, representative immunoblot) were calculated as

701 MAVS:β-actin ratios and expressed as fold change from un-treated, un-infected controls. Data  
702 are mean ± SEM,  $n = 6$ ,  $*P \leq 0.05$  versus infected, scramble treated Air or Smk controls. (D)  
703 Virus replication was assessed. Data are mean ± SEM,  $n = 6$ ,  $*P \leq 0.05$  versus infected,  
704 scramble-treated controls. Statistical differences were determined with one-way ANOVA  
705 followed by Bonferroni post-test.  
706

Figure 7



707

708 **Fig. 7.** Roles of miR-125a and b in the regulation of inflammatory and antiviral responses in

709 IAV infection. Increased levels of miR-125a and b, for example in COPD, reduces the protein

710 expression of A20 that results in uncontrolled NF-κB activation, leading to exaggerated

711 induction of pro-inflammatory cytokines. miR-125a and b also targets and reduces MAVS and

712 antiviral type I and III IFN production. Inhibition of miR-125a and b enhances MAVS and

713 antiviral responses and suppresses viral infection.